Title

Active sensing and damage detection using piezoelectric zinc oxide-based nanocomposites

Journal

Nanotechnology, 24(18)

ISSN

0957-4484

Authors

Meyers, Frederick N
Loh, Kenneth J
Dodds, John S
et al.

Publication Date

2013-05-10

DOI

10.1088/0957-4484/24/18/185501

Peer reviewed

Active Sensing and Damage Detection using Piezoelectric Zinc Oxide-based Nanocomposites

Frederick N. Meyers[1], Kenneth J. Loh[2,*], John S. Dodds[3], Arturo Baltazar[4]
[1]Department of Mechanical & Aeronautical Engineering, University of California, Davis, CA 95616, USA
[2]Department of Civil & Environmental Engineering, University of California, Davis, CA 95616, USA
[3]Naval Surface Warfare Center, Crane, Fallbrook Detachment, Fallbrook, CA 92028, USA
[4]Robotics and Advanced Manufacturing Program, CINVESTAV, Carretera Saltillo-Monterrey Ramos Arizpe, Coah, México 25900

[*]Corresponding e-mail: kjloh@ucdavis.edu

Abstract. This study investigated the design and performance of piezoelectric nanocomposite-based interdigitated transducers (IDTs) for active sensing and damage detection. First, thin films that are highly piezoelectric and mechanically flexible were designed by embedding zinc oxide (ZnO) nanoparticles in a poly(vinylidene fluoride-trifluoroethylene) (PVDF-TrFE) piezo-polymer matrix. Second, the suspended nanoparticle solutions were then spin coated onto patterned comb electrodes to fabricate the IDTs. The films were then poled to align their electric domains and to increase their permanent piezoelectricity. Upon IDT fabrication, its sensing and actuation of Lamb waves on an aluminum pipe was validated. These results were also compared to data obtained from commercial Macro Fiber Composite IDT transducers. In the last phase of this work, damage detection was demonstrated by mounting these nanocomposite sensors and actuators (using a pitch-catch setup) onto an aluminum pipe and plate. Damage was simulated by tightening a band clamp around the pipe and by drilling holes in the plate. A damage index calculation was used for comparing results corresponding to different levels of damage applied to the plate (*i.e.*, different drilled hole depths), and good correlation was observed. Thus, ZnO/PVDF-TrFE transducers were shown to have the potential for being used as piezoelectric transducers for structural health monitoring and damage detection.

1. Introduction

Piezoelectric materials have been demonstrated as an effective tool for damage detection and structural health monitoring (SHM). Due to the fact that piezoelectric materials can generate an electric field in response to dynamic strain (*i.e.*, the direct piezoelectric effect) and a strain in response to an electric field (*i.e.*, the converse piezoelectric effect), they can be used as both sensors and actuators, respectively. The sensitivity of these sensors and actuators is described by its piezoelectric coefficient, which determines the magnitude of the electric field produced by a sensor or the amount of strain generated by an actuator. Common materials with high piezoelectric coefficients include piezo-ceramics such as lead zirconate

titanate (PZT). They are inherently brittle, so an alternative is to use flexible piezo-polymers (typically with lower piezoelectricity) such as poly(vinylidene fluoride) (PVDF) and its trifluoroethylene copolymer (PVDF-TrFE). These piezoelectric transducers have been instrumented onto various types of structures for detecting damage such as cracks in metallic structures [1], loose bolts in structural member connections [2], and delamination in fiber-reinforced polymer composites [3], among others [4-6]. For example, crack propagation generates high frequency vibrations, or acoustic emissions, that can be measured by piezoelectric sensor networks [7]. Instead of using them as passive sensors, piezoelectric materials also have the unique ability to actuate and interrogate the structure. One can command it to generate ultrasonic vibrations which then propagate in the structure, and the characteristics of damage can be identified through analysis of measured response signals [8].

Piezoelectric actuators, when excited by a high-voltage alternating current (AC) excitation, can generate surface acoustic waves, or Rayleigh waves. Rayleigh waves propagate outward from an actuator, in all directions, and through the material body. When confined to a plate of finite thickness, they are known as Lamb waves. Lamb waves, when confined to geometries such as a plate strip or pipe, are guided by these structural geometries and take advantage of internal reflections to travel relatively long distances. In addition, Lamb waves scatter when they encounter any changes in boundary conditions, changes in material properties, and especially damage (*e.g.*, a crack). Measuring changes in the properties of scattered waves using piezoelectric sensors allows one to detect, quantify, and even localize damage [9].

In general, two different strategies can be adopted for Lamb wave-based damage detection, namely pitch-catch or pulse-echo. A pitch-catch strategy requires at least one piezoelectric actuator and another sensor. The actuator is commanded to propagate Lamb waves, and the response signals are measured by the sensors positioned elsewhere in the structure [10]. Changes in the response signal's time- and frequency-domain properties can be correlated to the severity and/or location of structural damage (particularly if a dense network of sensors and actuators are employed). In contrast, a pulse-echo setup typically uses the same piezoelectric transducer as both the actuator and sensor. In this case, the actuation signal is a short pulse to generate a pulse-like Lamb wave. Upon generating the actuation signal, the piezoelectric transducer then senses the response signal, which in this case is the Lamb wave "echo" after it reflects due to structural boundary conditions and/or structural damage [11]. Pitch-catch arrays experience less attenuation over the same spatial domain because the signal does not need to reflect off an edge or other boundary condition to be detected. On the other hand, a pulse-echo setup reduces costs by combining the roles of sensor and actuator. For both cases, one can actively interrogate the structure for on-demand SHM, as opposed to relying on passive sensors that record the response of structures due to ambient environmental excitations.

Many researchers have demonstrated that PZT sensor and actuator networks are able to detect damage in various types of structures (*e.g.*, composites, reinforced concrete, and metallic structures, to name a few). For example, Sohn *et al.* [12] showed that PZT transducers can generate Lamb waves and detect delamination in a fiber-reinforced polymer (FRP) composite test structure. Wang *et al.* [13] measured debonding between steel reinforcement bars and concrete by embedding piezoelectric transducers within the structure. In addition to interfacial damage, Lamb waves are also useful for sensing damage in steel (or metallic) structural members [14]. However, signal processing methods are needed to successfully identify damage (*i.e.*, its type, severity, and location). Damage severity can be quantified by examining the root-mean-square deviation from a baseline signal [15]. Damage can also be mapped using time and frequency analyses in conjunction with an array of sensors [16]. While pitch-catch techniques are extremely useful, Giurgiutiu *et al.* [17] showed that detection of close range (<100 mm) damage was more effective by measuring the impedance of PZTs. Even with an arsenal of signal processing tools and diagnostic techniques, there exist some limitations. PZT is one of the most commonly used piezoelectric materials, but it is a brittle ceramic that cannot couple to certain structures and geometries (*e.g.*, curved pipes). Poor coupling between the piezoelectric transducer and structure reduces its damage detection

effectiveness, especially at longer distances [18]. In addition, because PZT is a lead-based material, it poses a possible environmental risk.

On the other hand, PVDF-TrFE is a piezoelectric polymer that possesses unique advantages as compared to PZTs. PVDF-TrFE is extremely flexible, thereby allowing it to conform to complex structural surfaces and geometries. When annealed above its Curie temperature, PVDF-TrFE naturally forms the β-phase, which exhibits higher piezoelectricity than its other morphologies [19]. PVDF-TrFE has found its way into various applications where flexible materials are desired, including medical ultrasounds [20] and tactile sensors [21]. Monkhouse *et al.* [22] produced interdigitated transducers (IDT) from PVDF-TrFE. These IDTs successfully propagated Lamb waves in an aluminum substrate, thus showing their usefulness for SHM applications. Although PVDF-TrFE has gained popularity, its piezoelectric coefficient is far lower than that of PZTs. The poor sensitivity of PVDF-TrFE has become a roadblock for some applications and has caused researchers to turn to developing piezoelectric composites, including ones such as PVDF-TrFE/nanotube blends [23], PZT-based mixes [24], and others [25-27].

One particular strategy for attaining materials with high piezoelectricity and mechanical flexibility is to assemble PVDF-TrFE-based nanocomposites. Among the diverse nanomaterials available today, zinc oxide (ZnO) is a low cost and readily available material with a fairly high piezoelectric coefficient. Many types of ZnO nanostructures, including nanowires, nanosprings, and nanospheres have been successfully produced by Wang [28] and others [29-31]. Interest in ZnO and its inherent piezoelectricity has led to the development of various devices, including an array of ZnO nanowires for energy harvesting [32] and ZnO thin films for surface acoustic wave transducers [33]. Moreover, the need for flexible and highly piezoelectric materials has motivated previous work by Dodds *et al.* [34] to create and enhance PVDF-TrFE nanocomposites using ZnO nanoparticles. It was shown that these ZnO/PVDF-TrFE nanocomposites were flexible and possessed greater piezoelectricity than pristine PVDF-TrFE; increasing ZnO concentrations increased its piezoelectricity. Furthermore, lower poling voltages could be used to achieve comparable piezoelectricity when PVDF-TrFE thin films were enhanced with ZnO nanoparticles. Continued work also showed that ZnO/PVDF-TrFE nanocomposite sensors successfully measured hammer impact vibrations and strains of a vibrating cantilevered beam [35]. While previous work validated the piezoelectricity and sensing performance of ZnO/PVDF-TrFE thin films, additional research is still needed to characterize their actuation and damage detection capabilities.

The goal of this study is to design ZnO/PVDF-TrFE IDTs and to validate their actuation and sensing of Lamb waves for detecting simulated damage in metallic plates and pipes. First, spin coating and photolithography have been used for fabricating ZnO/PVDF-TrFE IDTs. Second, high voltage poling has been performed to align their electric domains, thereby enhancing their piezoelectricity. Then, sensors and actuators have been instrumented onto an aluminum pipe, and a pitch-catch setup has been used to validate the actuation and sensing of Lamb waves. Finally, damage detection tests have been conducted on the same pipe, as well as on an aluminum plate. Damage has been simulated by tightening a band clamp around the pipe or by drilling different sized holes in the plate. Results from these experiments validate the use of ZnO/PVDF-TrFE for future development and SHM applications.

2. Nanocomposite Transducer Fabrication

In this study, IDTs that incorporated ZnO/PVDF-TrFE were designed and fabricated. The results from various validation tests (as will be explained later) were compared to data obtained from commercial Macro Fiber Composite (MFC) IDTs (M-4010-P1 piezoelectric transducers from Smart Materials). In general, IDTs combine two interlocking comb-shaped electrodes and a third grounding electrode. IDTs are useful for propagating Lamb waves using thin film piezoelectric materials and have been shown to be more effective than comb patterns or square electrodes. Bellan *et al.* [36] showed that the resonant

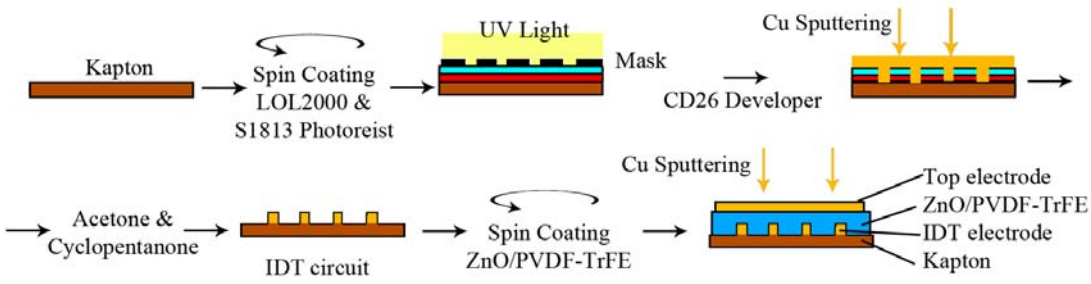

Figure 1: The ZnO/PVDF-TrFE interdigitated transducer fabrication process is shown here. Kapton was used as the flexible substrate. Then, a photolithographic process was used to deposit the IDT electrodes, followed by spin coating the nanocomposite. The final step was sputtering a top copper electrode and then poling the film.

frequency of the transducer can be controlled by the IDT finger spacing. In addition, actuation was more effective when each separate comb was driven by signals of opposite polarity, which doubled the voltage difference between fingers.

Prior to fabricating the nanocomposite, an IDT circuit was designed using CAD software and a pattern generator, and photolithography was used to create the IDT electrodes on a Kapton (Dupont) substrate (figure 1). Kapton was chosen for its mechanical robustness, flexibility, and chemical inertness. First, the pattern generator exposed a photosensitive glass mask to create a highly detailed circuit for the photolithographic process. The electrode finger spacing (*i.e.*, 0.9 mm) was chosen to be the same as the commercial or control MFC transducers to keep results analogous. Second, once exposed, the mask was developed in a clean room using CD-26 aqueous developer. The result was a glass mask with the desired IDT pattern. Thirdly, Kapton substrates were prepared by spin coating an LOL2000 lift-off-layer, followed by annealing. The process continued with spin coating S1813 photoresist and another annealing step. After annealing, the glass mask was placed on the Kapton substrates and exposed to ultraviolet (UV) light. The exposed films were then developed using CD-26 developer and washed in deionized water. It should be mentioned that using both a lift-off-layer and photoresist improved the quality of the circuit by undercutting the layers and provided a suitable surface for the metal electrodes. Finally, 250 nm of copper was sputtered to form the electrodes. Unexposed photoresist and the associated excess copper were removed using acetone, and the remaining LOL2000 was removed by cyclopentanone. It should be mentioned that copper was selected since it was readily accessible, and other metals would also suffice. Figure 2 shows a completed IDT electrode deposited onto the Kapton substrate.

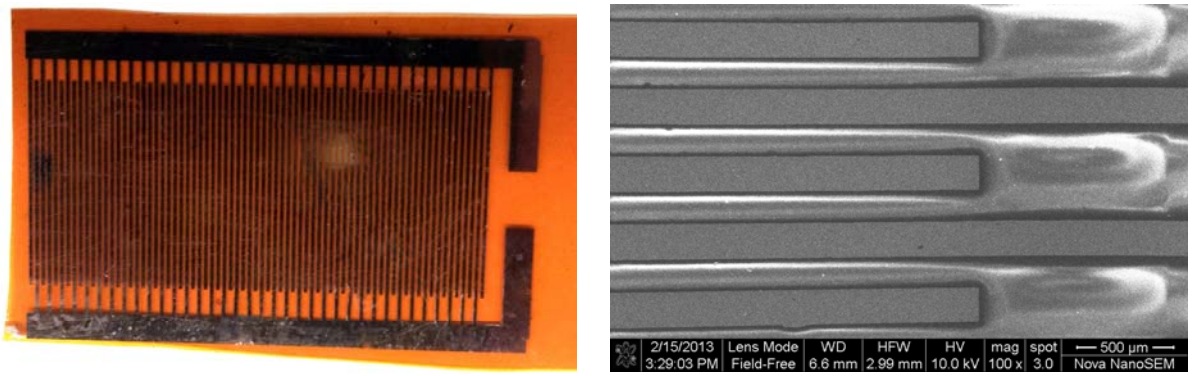

(a) (b)

Figure 2: (a) The designed IDT circuit was patterned and deposited onto a flexible Kapton substrate. **(b)** An SEM image detailing the IDT deposition, verifying that the process worked as expected, and there were no shorts between fingers.

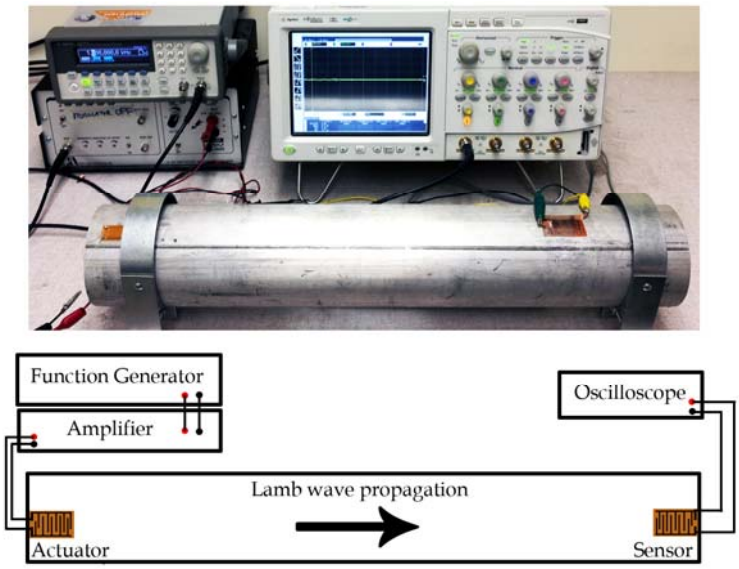

Figure 3: Validation of nanocomposite sensing and actuation was performed using an aluminum test pipe structure. The sensor and actuator were mounted onto opposite ends of the pipe. A function generator and high-voltage amplifier were used to generate Lamb waves with the actuator, and a digital oscilloscope was connected to the sensor for data acquisition.

After the patterning and deposition of IDT electrodes, a ZnO/PVDF-TrFE nanocomposite was spin coated on top using a Laurell spin processor. The nanocomposite solution was first prepared by dissolving PVDF-TrFE in methyl ethyl ketone (MEK) by stirring the mixture at 50 °C. Second, ZnO nanoparticles (20 nm spheres from Nano Armor) were added to obtain a 10 *wt.*% solution. Since ZnO is not soluble in MEK, the solution was bath ultrasonicated (135 W, 42 kHz) for 180 min to obtain a homogenous suspension. It should be mentioned that a 10 *wt.*% ZnO/PVDF-TrFE solution was used because this concentration can be readily suspended by ultrasonication, and previous characterization studies showed their high remnant polarization and piezoelectricity [34]. Higher concentrations are possible, but films become brittle, and solutions have a shorter shelf life due to reagglomeration of ZnO. To spin coat the nanocomposite, a small amount of nanomaterial solution was pipetted onto the IDT-Kapton surface. The substrate was spun at 500 RPM for 5 s and then followed by 1,600 RPM for 25 s. These steps ensured even spreading and thinning of the solution over the entire substrate. The specimens were then annealed at 140 °C for 2 h, which produced a 15 µm-thick nanocomposite (as measured using a Dektak profilometer). Finally, a grounding electrode (250 nm of copper) was sputtered on top of the ZnO/PVDF-TrFE film. This procedure completed the ZnO-based IDT fabrication (figure 1). At this stage, electrical domains in the nanocomposite were randomly distributed and would produce low bulk film piezoelectricity. Thus, high voltage direct current (DC) poling was performed using a DC power supply and UltraVolt amplifier applying an electric field of 50 MV-m^{-1} across the thickness of the specimen. During poling, samples were kept at 70 °C and then slowly cooled to increase the effectiveness of the poling process [37].

3. Sensing and actuation

ZnO/PVDF-TrFE nanocomposite IDTs were shown to sense and actuate Lamb waves as a prerequisite for damage detection and SHM. Sensing and actuation were demonstrated using an aluminum pipe (600 mm long, 6 mm thick, with an inner diameter of 88 mm) as a waveguide and test structure (figure 3). First, a frequency sweep was performed to determine the driving signal parameters that yielded the largest signal-

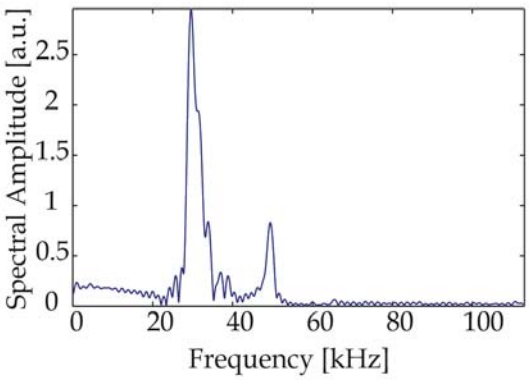

Figure 4: The frequency response, as measured by a ZnO/PVDF-TrFE sensor, is shown. The peak seen at 30 kHz was taken as the optimum operating frequency that provided the greatest signal-to-noise ratio for sensing and actuation.

to-noise (SNR) ratio. Second, MFC commercial transducers were used to actuate Lamb waves, and ZnO/PVDF-TrFE IDTs were employed as sensors (section 3.1). Finally, the roles were reversed in section 3.2, and ZnO/PVDF-TrFE actuators generated Lamb waves in the test pipe; commercial MFC IDTs recorded the response.

3.1 Sensing validation

Sensor and actuator SNR is dependent on the excitation frequency, and the response may not be measured with sufficient resolution if the driving frequency exceeds its intrinsic operating bandwidth. Thus, the first step was to utilize a pitch-catch setup to determine the spectral response of an MFC and ZnO/PVDF-TrFE system. An MFC transducer and nanocomposite IDT were attached to opposite ends of the aluminum pipe using a cyanoacrylate adhesive as shown in figure 3. The MFC IDT was used as the actuator for validating the sensing performance of ZnO/PVDF-TrFE sensors. Here, the actuation signal was a six-period 200 Vpp Hamming signal generated by an Agilent 33250A function generator and amplified using an AA Lab Systems A-303 amplifier. This signal was pulsed every 200 ms to actuate MFC transducers, thereby producing Lamb waves in the pipe. These Lamb waves were measured using ZnO/PVDF-TrFE sensors (located 300 mm away) and recorded using an Agilent MSO8104A mixed-signal digital oscilloscope. The frequency of the actuation signal was varied from 6 to 120 kHz in 6 kHz increments. Data was recorded for each excitation frequency, and a Fast Fourier Transform (FFT) was calculated using MATLAB.

The results from the pitch-catch frequency sweep tests were summarized by taking the FFT for each different excitation frequency and linearly averaging the plots to obtain an overall spectral response as shown in figure 4. Figure 4 shows a maximum at 30 kHz and a relative peak at 50 kHz. These results show that the optimum SNR was achieved when the system was operated at 30 kHz. The source of the second peak at 50 kHz was not thoroughly analyzed, but it was possibly due to the interactions between the resonant frequencies of the sensor, actuator, and test structure. In essence, the purpose of this analysis was to find the best SNR conditions, rather than to determine fundamental frequencies or Lamb wave dispersion curves. It should be mentioned that optimizing the driving signal is especially important since the measured response amplitude can be small (<1 mV), depending on the distance between the sensor/actuator pair.

In addition to the frequency response, the time-domain results were also examined for sensing validation. Here, the MFC was actuated at 30 kHz (six periods) to demonstrate that the nanocomposites measured the

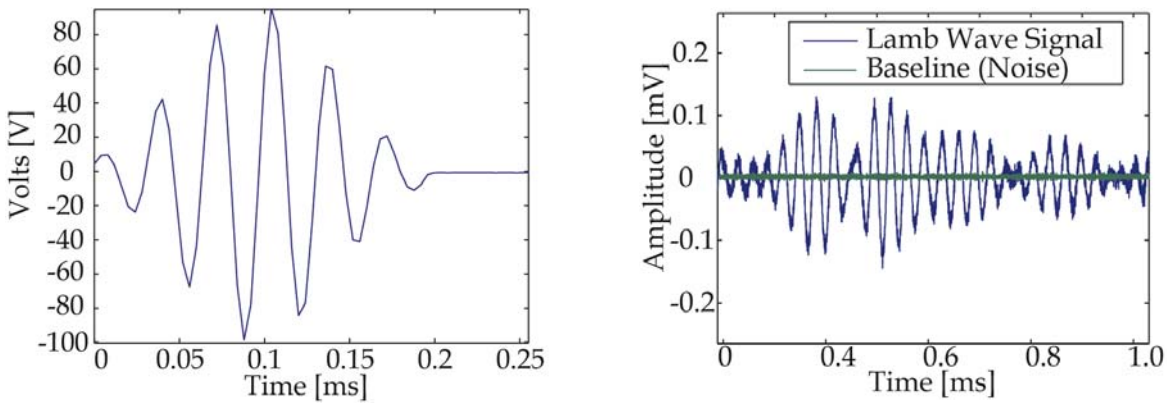

(a) (b)

Figure 5: (a) The input actuation signal was a 200 Vpp six-period 30 kHz sine Hamming signal. **(b)** The generated Lamb wave was measured by a ZnO/PVDF-TrFE sensor, and the voltage time history shows successful lamb wave detection.

generated Lamb waves. The excitation signal is shown in figure 5a, and it was pulsed every 200 ms. The pulsed actuation signal was employed so that the sensor could measure multiple responses corresponding to the same setup/case. The pulse delay of 200 ms was selected so that the Lamb waves had sufficient time to attenuate before the next wave was generated. Similar to before, the nanocomposite sensor was connected to an Agilent oscilloscope for data acquisition.

Figure 5b shows a representative voltage time history plot as measured by the ZnO/PVDF-TrFE IDTs, along with a baseline (no excitation) signal. It can be seen that the sensor successfully measured the propagated Lamb wave. In addition, multiple reflections off of the pipe boundaries were also recorded. It should be noted that edge effects were a potential source scattering and interference, but it is still possible to resolve individual wave packets and to note their visual similarities to the input actuation signal (figure 5a). These waveform characteristics support the validation of Lamb wave sensing. Also plotted in figure 5b is the baseline signal measured by the ZnO/PVDF-TrFE IDT when there were no excitations or Lamb waves generated. The average root-mean-square (RMS) noise level was approximately 2.5 μV, which was significantly smaller than the sensed signal shown in figure 5b. Overall, the sensor exhibited high SNR and was sufficient to resolve the measured Lamb waves.

3.2 Actuation validation

The ZnO/PVDF-TrFE IDTs were also validated for their actuation capabilities by propagating Lamb waves in the aluminum pipe. The experimental setup was similar to section 3.1 and figure 3, except that the nanocomposite was the actuator, and the MFC was used as the sensor. The same actuation signal was used (figure 5a). It was verified that the actuation signal propagated Lamb waves in the pipe, and the response was sensed by the MFC transducer; its voltage output was recorded using the Agilent oscilloscope as before. Figure 6a shows a typical voltage time history response as measured by the MFC. Similar to the results shown in figure 5b, individual wave packets can be seen, and the scattering effects are as expected. The similarities between figures 6a and 5b show that both sensing and actuation configurations using the ZnO/PVDF-TrFE IDTs were successful.

In addition to the actuation validation tests, the ZnO/PVDF-TrFE IDT was also tested to determine the distance of Lamb wave propagation. Here, the distance between the sensor and actuator was varied from

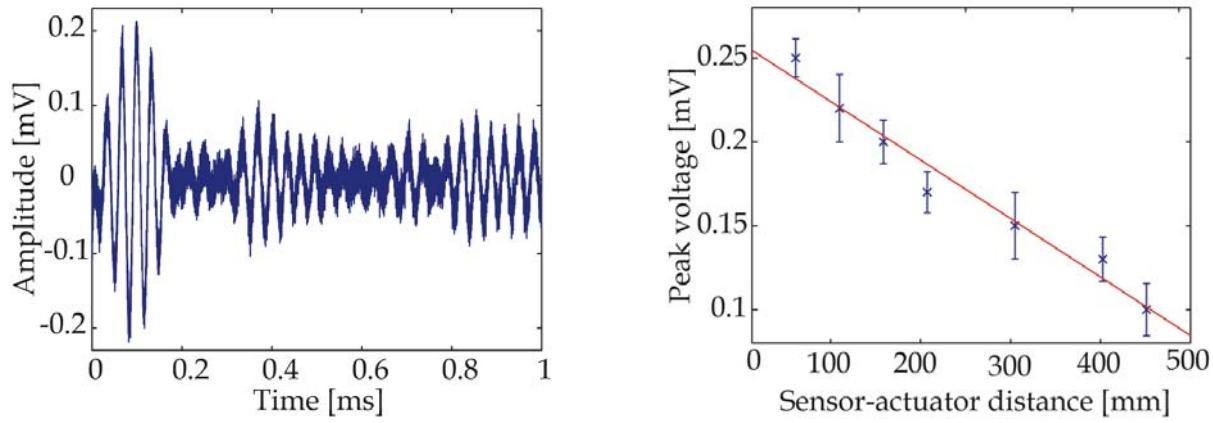

(a) (b)

Figure 6: (a) A ZnO/PVDF-TrFE was employed as the actuator and generated Lamb waves in the aluminum pipe. An MFC sensor measured the response, and the voltage time history response is shown here. **(b)** The distance between the sensor and actuator was varied from 50 to 450 mm, and the peak voltage measured by the sensor decreased in a linear fashion.

50 to 450 mm (in 50 mm increments) by adjusting the position of the MFC. At each step, the actuator was excited by the same signal to propagate Lamb waves, and the MFC sensed the response. The results are summarized in figure 6b, which shows the change in the voltage time history's peak amplitude as a function of the distance between the sensor and actuator. The peak amplitude of the signal decreased only 0.15 mV as the MFC sensor was moved from 50 to 450 mm. This result confirms that the ZnO/PVDF-TrFE IDTs were capable of propagating Lamb waves over long distances.

It should be noted that the voltage output from ZnO/PVDF-TrFE transducers was much smaller than that from the MFC. This is expected, because MFC transducers use PZT, which is a material that exhibits much higher piezoeletricity. In addition, the thicknesses of the two types of transducers were not comparable, which contributed to the generation of different signal amplitudes. The MFC transducer used was on the order of 100 µm thick, whereas the nanocomposite thin films were ~15 µm thick. Nevertheless, MFC proved to be a good comparison and for use as a control device due to its commercial availability and proven consistency.

4. Damage Detection

As discussed in section 1, it is possible to quantify damage using Lamb waves and active sensing. In this section, a pitch-catch setup was employed to test the ability of ZnO/PVDF-TrFE transducers to detect the presence of damage in test structures such as an aluminum pipe and plate. The procedure began by using the ZnO/PVDF-TrFE to generate Lamb waves and then recording the baseline signal using an MFC. Next, damage was introduced to the structure and active sensing was performed again. The time- and frequency-domain signals were then analyzed to quantify damage.

4.1 Damage Index

In a pitch-catch setup, Lamb waves are generated by a piezoelectric actuator and measured by a sensor some distance away. If damage (*i.e.*, a crack, hole, or change in material properties) is in the path of Lamb wave propagation, then scattering occurs. The sensor then picks up the scattered waves, and the output

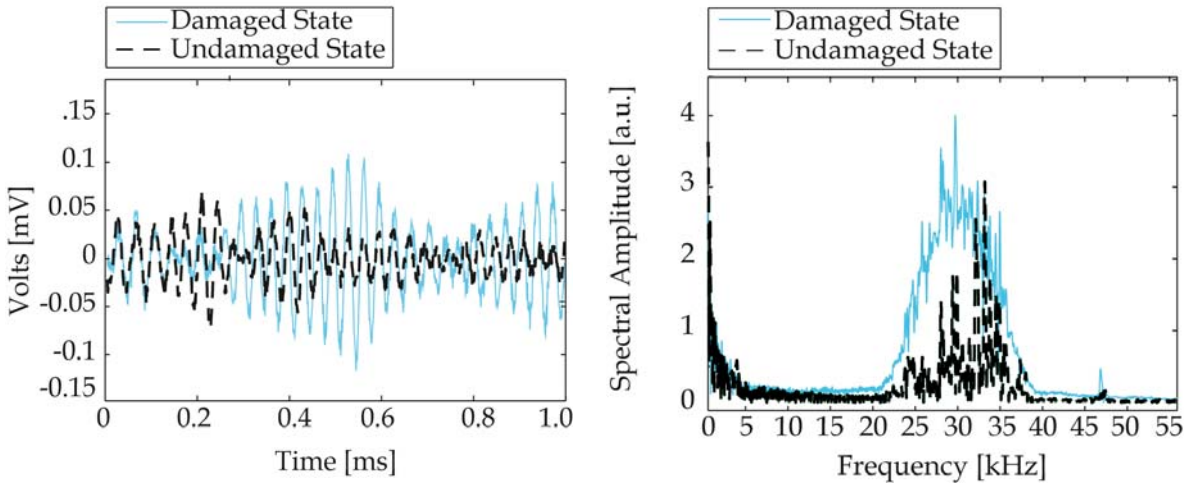

(a) (b)

Figure 7: (a) The voltage time history corresponding to an undamaged case is overlaid with one measured when damage was applied to the pipe structure (*i.e.*, using a band clamp). **(b)** The corresponding frequency-domain results for the undamaged and damaged cases are shown.

can be measured as a voltage time history signal. By comparing the scattered waveform to a previously measured baseline state, one can estimate the severity of damage. Monnier *et al.* [38] showed that comparing the spectral amplitudes of scattered and baseline states was a useful metric for damage detection. In this way, a baseline FFT can be calculated and compared to another state to quantify damage. The difference between states is referred to as the damage index (DI) and is expressed as:

$$DI = \sum_{i=1}^{n} |F_i - FD_i| \Big/ \sum_{i=1}^{n} |F_i| \tag{1}$$

where F_i is the i^{th} FFT coefficient of the baseline signal, and FD_i is the i^{th} coefficient of the damaged Fourier spectrum. In other words, the damage index calculates the normalized difference between the spectral amplitudes of the two states at each frequency. In this way, the amount of damage is expressed as a change in the spectral properties of the signal with respect to its original baseline.

4.2 Simulated pipe damage

The first damage detection validation was performed on an aluminum pipe. Damage was simulated by tightening a band clamp around the pipe and at a location between the MFC sensor and ZnO/PVDF-TrFE actuator, thereby causing stress and changes in geometry. The band clamp was selected as the means for simulating damage because damage could be added or removed between experiments without compromising structural integrity. Similar to section 3, the MFC and nanocomposite IDTs were placed on opposite ends of the pipe and 300 mm apart. A 200 Vpp 30 kHz signal (figure 5a) was used to actuate the nanocomposite. The signal for the baseline case (without damage) was first collected. Then, the band clamp was tightened around the center of the pipe, and measurements were repeated.

Figure 7a plots an overlay of a representative voltage time history of a baseline case and another damaged scenario. It should be mentioned that a total of seven sets of tests were conducted, but only one representative undamaged/damaged case is presented here. It can be observed from figure 7a that damage caused a change in the measured waveform shape and amplitude. FFT was then performed on the time-domain measurements, and figure 7b reveals the differences in spectral properties between the

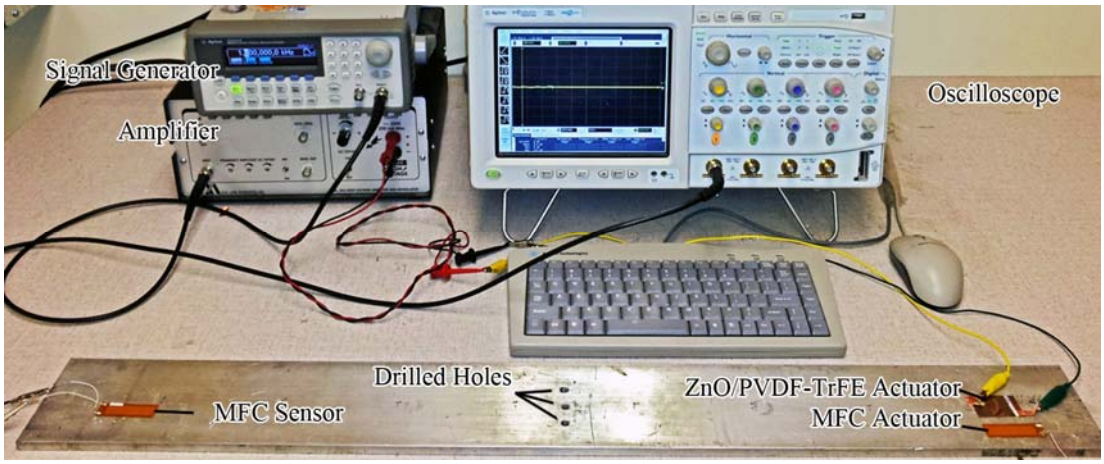

Figure 8: The experimental setup for the plate damage detection study is shown. The MFC on the left served as the sensor, while the ZnO/PVDF-TrFE actuator was instrumented on the opposite end. An MFC actuator was also affixed to the plate for comparison purposes.

undamaged and damaged cases. The difference in the signals was due to two effects caused by the band clamp. First, Lamb waves were scattered by a change in the boundary condition, since the clamp was in direct contact with the pipe. Second, the clamp induced stresses, which changed the Lamb wave propagation characteristics. The measured response signal, as shown in figure 7a, manifested itself as reflections, changes in amplitude, and phase shifting. These distortions also clearly affected the frequency spectrum, as can be seen in figure 7b.

The DI was then computed using equation 1 and the undamaged/damaged spectral data, and the averages (and standard errors of the mean) are shown in table 1. The results shown in table 1 were computed using seven sets of test data. First, one can see that the baseline DI is 0.050 ± 0.006. As expected, this number is close to zero, thus verifying that the frequency spectrum does not change when there is no damage. The baseline DI is not exactly zero due to changes in the baseline signal caused by manual placement of the transducers, which created small deviations in the precise location of the actuator. Second, it can be observed from table 1 that the DI for the damaged case is 0.564 ± 0.020. The DI is significantly more than an order of magnitude higher than the baseline DI, thus indicating successful damage detection. It should be mentioned that multiple ZnO/PVDF-TrFE IDTs were used in this damage detection validation study to ensure similar and consistent measurements. However, slight differences in the manual manufacturing process could cause variations from specimen to specimen; the result is that the frequency domain properties could change depending on the fabrication batch. Therefore, it is important to compare baseline and damaged results on a specimen-by-specimen basis, which was done in this study.

4.3 Plate damage

In addition to the pipe experiments, damage detection validation tests were also performed using an aluminum plate (888 mm long, 100 mm wide, and 10 mm thick). An MFC sensor and a ZnO/PVDF-TrFE

Table 1: Damage index results for an aluminum pipe damaged due to applied stresses from a band clamp.

	Average DI	**Standard error of the mean**
Undamaged (baseline)	0.050	0.006
Damaged (band clamp)	0.564	0.020

Table 2: Damage index results for an aluminum plate damaged due to applied stresses from a c-clamp.

	Average DI	Standard error of the mean
DI (ZnO/PVDF-TrFE actuator)	0.128	0.002
DI (MFC actuator)	0.130	0.001

actuator were instrumented at opposite ends of the plate and approximately 650 mm apart (figure 8). Another MFC IDT was also instrumented for use as an actuator for comparison purposes. For both cases, the same actuation signal shown in figure 5a was used. A c-clamp applied to the center of the plate was used to induce repeatable and nondestructive damage to the plate. Handle rotations were counted in order to tighten the clamp in a consistent fashion.

A total of seven sets of tests were conducted, and the DI was calculated and summarized in table 2. One can see from table 2 that the average DI, when using ZnO/PVDF-TrFE IDTs as the actuator, was very similar to that when the MFC was employed for actuation. One can compare the results shown in table 2 to table 1 and see that the standard error is much smaller for the pipe experiment. This is likely because the c-clamp was much easier to tighten and remove between experiments (as compared to the hose clamp), thus producing more consistent measurements. This result verifies that, like the MFCs, the ZnO-based transducer was capable of interrogating the structure, and the system detected damage in the plate. Moreover, the spectral properties changed for both MFC and ZnO/PVDF-TrFE actuators (similar to figure 7b), which indicate that the DI is measuring changes in the Lamb waves and not changes in the actuators.

It was also desirable to measure actual damage, in addition to induced stress from the applied c-clamp. To accomplish this, a 3/8th-inch (9.5 mm) bit was used to drill a progressively deeper hole through the center of the plate (*i.e.*, in 1 mm increments). The purpose of a drilled hole was to create residual stresses and changes in geometry that scatter Lamb waves (and simulate actual damage in the structure). The DI was calculated each time the hole was drilled 1 mm deeper into the plate. In addition, after the first hole was drilled through, a second hole was drilled 25 mm away and parallel to the midplane. This was followed by a third hole in the opposite direction; the DI was also determined after each of these additional drilled holes. Figure 8 shows the experimental setup, and figure 9 plots the calculated DI results as a function of hole depth. It can be seen from figure 9 that the damage index increases consistently with the depth of the drilled hole. This result confirms that the ZnO/PVDF-TrFE active sensing strategy and the damage index method are capable of capturing not just the presence of damage but also its severity. In addition, when more holes were present in the structure, drastic changes in the DI were seen (figure 9). It should also be mentioned that the control case (*i.e.*, using an MFC as the actuator) demonstrated a similar result (figure 9), thus verifying the conclusions drawn by the nanocomposite actuator. It also appears that the ZnO-based nanocomposite was more sensitive to damage than the MFC (based on greater changes in DI with more severe damage introduced to the structure). All in all, these results validate the use of ZnO/PVDF-TrFE IDTs for actuation, sensing, and damage detection. It should be mentioned that this is only a preliminary study demonstrating their potential for SHM and damage detection. More in-depth characterization and SHM implementation studies will be conducted in the near future.

5. Conclusions

In this study, ZnO/PVDF-TrFE interdigitated transducer sensors and actuators were designed and fabricated for SHM and damage detection applications. Previous work showed that ZnO nanoparticles enhanced the remnant polarization and piezoelectricity of pristine PVDF-TrFE piezoelectric polymers. Thus, the objective of this work was to characterize and validate ZnO/PVDF-TrFE IDT sensing and

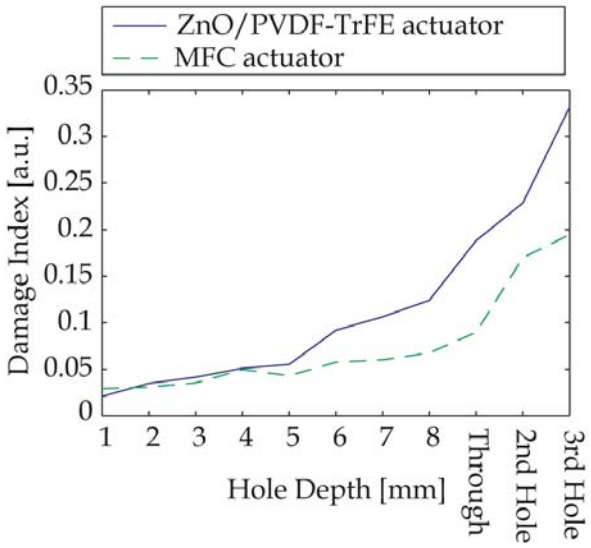

Figure 9: Damage was introduced to an aluminum plate by drilling progressively deeper holes and additional through-holes at different locations. Damage detection experiments were conducted, and the damage index was found to increase in tandem with greater damage applied to the structure.

actuation performance. First, an IDT electrode pattern was deposited onto a Kapton substrate using a photolithographic process. Second, ZnO nanoparticles were suspended in a PVDF-TrFE solution using bath ultrasonication and then spin coated onto the IDT-Kapton substrate. Then, Lamb wave sensing and actuation validation tests were demonstrated on an aluminum pipe using commercial MFC transducers for comparison. It was confirmed that the ZnO/PVDF-TrFE IDTs were able to propagate Lamb waves (*i.e.*, when excited by a high-voltage six-period Hamming sine signal). Also, they were able to detect and record Lamb waves generated by commercial MFC transducers.

Upon validation of its sensing and actuation performance, damage detection tests were conducted using the same aluminum pipe and also a plate structure. Repeatable damage (in the form of applied stresses) was introduced to the pipe and plate using clamps. In later tests, progressively deeper holes were also drilled in the plate to inflict actual damage. In all these cases, ZnO/PVDF-TrFE IDTs were instrumented onto the structure and served as actuators, while commercial MFC transducers measured the response signals. A damage index method was employed to quantify the severity of damage. The results from these tests showed that the prototype sensor/actuator, when combined with this damage index method, was able to quantify the severity of damage. The results from using ZnO/PVDF-TrFE IDTs were also comparable when MFCs were used as actuators (*i.e.*, the control case). Although the ZnO/PVDF-TrFE transducers produced a smaller voltage output than MFCs, its advantage is its low poling voltage requirement, simple manufacturing process, and low cost. This study demonstrated that ZnO/PVDF-TrFE nanocomposite transducers are viable for damage detection and SHM. Future work will entail more in-depth characterization studies, as well as their application in larger structures.

Acknowledgements

The authors thank the UC MEXUS-CONACYT program for the financial support of this research. The authors would also like to express their sincere gratitude to the staff of the Northern California Nanotechnology Center (NC^2) for their assistance with photolithography processes, as well as Mr. Donghyeon Ryu for assisting with SEM imaging. Dr. Valeria La Saponara is also acknowledged for providing access to her equipment for laboratory testing.

References

[1] Tua, P., Quek, S. and Wang, Q., "Detection of Cracks in Plates Using Piezo-Actuated Lamb Waves," Smart Materials and Structures, **13**(4), 643 (2004).

[2] Doyle, D., Zagrai, A., Arritt, B. and Çakan, H., "Damage Detection in Bolted Space Structures," Journal of intelligent material systems and structures, **21**(3), 251-264 (2010).

[3] Guo, N. and Cawley, P., "The Interaction of Lamb Waves with Delaminations in Composite Laminates," The Journal of the Acoustical Society of America, **94**(4), 2240-2246 (1993).

[4] Staszewski, W., Tomlinson, G. and Boller, C., *Health Monitoring of Aerospace Structures*, Wiley Online Library: (2004).

[5] Seale, M.D., Smith, B.T. and Prosser, W., "Lamb Wave Assessment of Fatigue and Thermal Damage in Composites," The Journal of the Acoustical Society of America, **103**, 2416 (1998).

[6] Ryden, N., Park, C.B., Ulriksen, P. and Miller, R.D., "Lamb Wave Analysis for Non-Destructive Testing of Concrete Plate Structures," Proceedings of Proceedings of the Symposium on the Application of Geophysics to Engineering and Environmental Problems (SAGEEP 2003), San Antonio, TX, April, 6-10 (2003).

[7] Carter, D. and Holford, K., "Strategic Considerations for the Ae Monitoring of Bridges: A Discussion and Case Study," Insight, **40**(2), 112-116 (1998).

[8] Giurgiutiu, V., *Structural Health Monitoring with Piezoelectric Wafer Active Sensors*, Academic Press: (2008).

[9] Viktorov, I.A., *Rayleigh and Lamb Waves: Physical Theory and Applications*, Plenum press New York: (1967).

[10] Giurgiutiu, V., "Tuned Lamb Wave Excitation and Detection with Piezoelectric Wafer Active Sensors for Structural Health Monitoring," Journal of intelligent material systems and structures, **16**(4), 291-305 (2005).

[11] Mouritz, A., Townsend, C. and Shah Khan, M., "Non-Destructive Detection of Fatigue Damage in Thick Composites by Pulse-Echo Ultrasonics," Composites science and technology, **60**(1), 23-32 (2000).

[12] Sohn, H., Park, G., Wait, J.R., Limback, N.P. and Farrar, C.R., "Wavelet-Based Active Sensing for Delamination Detection in Composite Structures," Smart Materials and Structures, **13**(1), 153 (2003).

[13] Wang, C.S., Wu, F. and Chang, F.K., "Structural Health Monitoring from Fiber-Reinforced Composites to Steel-Reinforced Concrete," Smart Materials and Structures, **10**(3), 548 (2001).

[14] Park, S., Yun, C.B., Roh, Y. and Lee, J.J., "PZT-Based Active Damage Detection Techniques for Steel Bridge Components," Smart Materials and Structures, **15**(4), 957 (2006).

[15] Park, G., Sohn, H., Farrar, C.R. and Inman, D.J., "Overview of Piezoelectric Impedance-Based Health Monitoring and Path Forward," Shock and Vibration Digest, **35**(6), 451-464 (2003).

[16] Ihn, J.B. and Chang, F.K., "Pitch-Catch Active Sensing Methods in Structural Health Monitoring for Aircraft Structures," Structural Health Monitoring, **7**(1), 5-19 (2008).

[17] Giurgiutiu, V., Zagrai, A. and Bao, J.J., "Piezoelectric Wafer Embedded Active Sensors for Aging Aircraft Structural Health Monitoring," Structural Health Monitoring, **1**(1), 41-61 (2002).

[18] Cho, J., Anderson, M., Richards, R., Bahr, D. and Richards, C., "Optimization of Electromechanical Coupling for a Thin-Film PZT Membrane: II. Experiment," Journal of Micromechanics and Microengineering, **15**(10), 1804 (2005).

[19] Akdogan, E.K., Allahverdi, M. and Safari, A., "Piezoelectric Composites for Sensor and Actuator Applications," Ultrasonics, Ferroelectrics and Frequency Control, IEEE Transactions on, **52**(5), 746-775 (2005).

[20] Robert, M., Molingou, G., Snook, K., Cannata, J. and Shung, K.K., "Fabrication of Focused Poly (Vinylidene Fluoride-Trifluoroethylene) P(VDF-TrFE) Copolymer 40–50 Mhz Ultrasound Transducers on Curved Surfaces," Journal of applied physics, **96**(1), 252-256 (2004).

[21] Li, C., Wu, P.M., Lee, S., Gorton, A., Schulz, M.J. and Ahn, C.H., "Flexible Dome and Bump Shape Piezoelectric Tactile Sensors Using PVDF-TrFE Copolymer," Microelectromechanical Systems, Journal of, **17**(2), 334-341 (2008).

[22] Monkhouse, R., Wilcox, P. and Cawley, P., "Flexible Interdigital PVDF Transducers for the Generation of Lamb Waves in Structures," Ultrasonics, **35**(7), 489-498 (1997).

[23] Levi, N., Czerw, R., Xing, S., Iyer, P. and Carroll, D.L., "Properties of Polyvinylidene Difluoride-Carbon Nanotube Blends," Nano Letters, **4**(7), 1267-1271 (2004).

[24] Graz, I., Krause, M., Bauer-Gogonea, S., Bauer, S., Lacour, S.P., Ploss, B., Zirkl, M., Stadlober, B. and Wagner, S., "Flexible Active-Matrix Cells with Selectively Poled Bifunctional Polymer-Ceramic Nanocomposite for Pressure and Temperature Sensing Skin," Journal of applied physics, **106**(3), 034503-034503-034505 (2009).

[25] Wu, Y. and Feng, T., "Fabrication and Mechanical Reinforcement of Piezoelectric Nanocomposites with ZrO_2 Nanoparticles Embedded in Situ," Journal of Alloys and Compounds, **491**(1), 452-455 (2010).

[26] Lin, H.B., Cao, M.S., Zhao, Q.L., Shi, X.L., Wang, D.W. and Wang, F.C., "Mechanical Reinforcement and Piezoelectric Properties of Nanocomposites Embedded with ZnO Nanowhiskers," Scripta Materialia, **59**(7), 780-783 (2008).

[27] Zhao, Y., Loh, K.J. and Chang, D., "Piezoelectric and Mechanical Performance Characterization of ZnO-Based Nanocomposites," Proceedings of Proceedings of the 19th Analysis & Computation Specialty Conference, 12-15 (2010).

[28] Wang, Z.L., "Zinc Oxide Nanostructures: Growth, Properties and Applications," Journal of Physics: Condensed Matter, **16**(25), R829 (2004).

[29] Gao, P. and Wang, Z.L., "Self-Assembled Nanowire-Nanoribbon Junction Arrays of ZnO," The Journal of Physical Chemistry B, **106**(49), 12653-12658 (2002).

[30] Kong, X.Y. and Wang, Z.L., "Spontaneous Polarization-Induced Nanohelixes, Nanosprings, and Nanorings of Piezoelectric Nanobelts," Nano Letters, **3**(12), 1625-1631 (2003).

[31] Pan, Z.W. and Wang, Z.L., "Nanobelts of Semiconducting Oxides," Science, **291**(5510), 1947-1949 (2001).

[32] Wang, Z.L. and Song, J., "Piezoelectric Nanogenerators Based on Zinc Oxide Nanowire Arrays," Science, **312**(5771), 242-246 (2006).

[33] Hickernell, F.S., "Zinc-Oxide Thin-Film Surface-Wave Transducers," Proceedings of the IEEE, **64**(5), 631-635 (1976).

[34] Dodds, J.S., Meyers, F.N. and Loh, K.J., "Piezoelectric Characterization of PVDF-TrFE Thin Films Enhanced with ZnO Nanoparticles," Sensors Journal, IEEE, **12**(6), 1889-1890 (2012).

[35] Dodds, J.S., Meyersb, F.N. and Loh, K.J., "Enhancing the Piezoelectric Performance of PVDF-TrFE Thin Films Using Zinc Oxide Nanoparticles," Proceedings of Proc. of SPIE Vol, **8345**, 834515-834511 (2012).

[36] Bellan, F., Bulletti, A., Capineri, L., Masotti, L., Yaralioglu, G.G., Degertekin, F.L., Khuri-Yakub, B., Guasti, F. and Rosi, E., "A New Design and Manufacturing Process for Embedded Lamb Waves Interdigital Transducers Based on Piezopolymer Film," Sensors and Actuators A: Physical, **123**, 379-387 (2005).

[37] Kaura, T., Nath, R. and Perlman, M., "Simultaneous Stretching and Corona Poling of PVDF Films," Journal of Physics D: Applied Physics, **24**(10), 1848 (2000).

[38] Monnier, T., "Lamb Waves-Based Impact Damage Monitoring of a Stiffened Aircraft Panel Using Piezoelectric Transducers," Journal of intelligent material systems and structures, **17**(5), 411-421 (2006).